12th International Conference on Structural Analysis of Historical Constructions
SAHC 2020
P. Roca, L. Pelà and C. Molins (Eds.)

COLLABORATIVE USE OF DEM AND FEM FOR BRICK JOINT SPLITTING IN STRONG EARTHQUAKE GROUND MOTION

TOSHIRO MAEDA[1*], HIROMU TANAKA[2], MIKI SHIRAHASHI[1] AND BUN HIGASHIZAWA[1]

[1]Department of Architecture, Graduate School of Creative Science and Engineering,
Waseda University
3-4-1, Okubo, Shinjuku-ku, Tokyo, 1698555, Japan
e-mail: tmaeda@waseda.jp, www.tmaeda.sci.waseda.ac.jp (*corresponding author)

[2] Structural Design Department, Shimizu Corporation
2-16-1, Kyobashi, Chuo-ku, Tokyo 1048370, Japan
email: hiromu_tanaka@shimz.co.jp

Keywords: Brick wall, Wooden frame, Micro-tremor observation, Excitation test, FEM, DEM

Abstract. *Masonry structures constructed about one hundred and fifty years ago, in the era of the opening of Japan, have been recognized as industrial heritages. Many of them are masonry warehouses made of brick or stone walls framed by wood members. In this research, a two-story warehouse in Tomioka city, a mortar jointed brick masonry with wooden frame reinforcements, was studied for strong earthquake ground motion. Several vibration modes were identified by micro-tremor observations and excitation tests. The three-dimensional FE overall model was constructed and tuned for the distinctive vibration modes. Two DEM local models, one for bending at the center bottom of the wall treated by plane strain, and the other for shear at the upper corner of the wall by plane stress, were constructed to evaluate brick joint splitting. For both models, dynamic displacement response obtained by the three-dimensional FEM were specified at their peripheries via periphery blocks. At the center bottom of the wall, horizontally developing joint splitting in the section was evaluated. At the upper corners, obliquely proceeding joint splitting on the wall was evaluated. In these analyses, the specified displacements were calculated by the FE model for intact brick walls, regardless of the degrading status of the walls. Although this assumption will have to be justified, the results of DEM were consistent with the reported summary of past earthquake damages.*

1 INTRODUCTION

Masonry structures constructed just after the opening of the modern Japan, about one hundred and fifty years ago, have been recognized as industrial heritages. Many of them are masonry warehouses made of brick or stone walls framed by wood members. Though some of them are renovated for modern use, it is indispensable to preserve their original structures for their values. Our research can help renovation design of utilizing their original structural strength. We have been studying collapse mechanisms of masonry structures e.g., a dry masonry Angkor heritage prototype [1 and 2] and a mortar jointed brick chimney in Tokoname [3]. Our strategy constitutes measurements of micro tremor, validation of finite element or

discrete element models, and simulation for unexpected large disturbances.

At this time, a two-story warehouse in Tomioka city shown in Figure 1, a mortar jointed brick masonry with wooden frame reinforcements, was studied for strong earthquake ground motion. It has six bays in longitudinal ridge direction of 33.1 m and two bays in transverse span direction of 7.6 m and the height is 9.7 m. Several vibration modes were identified by micro-tremor observation and 2nd floor excitation, which were accompanied with remarkable out-of-plane deformation of walls. Taking these three-dimensional vibration characteristics into account, we decided to couple three-dimensional finite element analyses with our two-dimensional discrete element method (DEM) software.

The three-dimensional overall FE model was tuned for the distinctive vibration modes by closely evaluating stiffness of wooden structures at roof and 2nd floor levels. Analyses for static horizontal load and dynamic ground motion exhibited that the Von Mises stress was dominated at the centre bottom and at the upper corners of the longer wall in the excitation along the shorter edge direction. The former predominance implied the dominating bending stress and the latter the dominating membrane stress due to the constraining effects of the perpendicular shorter walls.

Two DEM local models were constructed; one for the centre bottom of the wall treated by plane strain and the other for the upper corner of the wall by plane stress. For both models, time-varying dynamic displacement response obtained by the three-dimensional FEM were specified at their peripheries. At the centre bottom of the wall, DEM revealed that the joint splitting was developing horizontally in the section; while at the upper corners, joint splitting was proceeding obliquely on the wall. In these analyses, FEM based overall response with intact brick walls was used regardless of the degrading status of the walls. Although this assumption will have to be justified, the results of DEM were consistent with the reported summary of past earthquake damages.

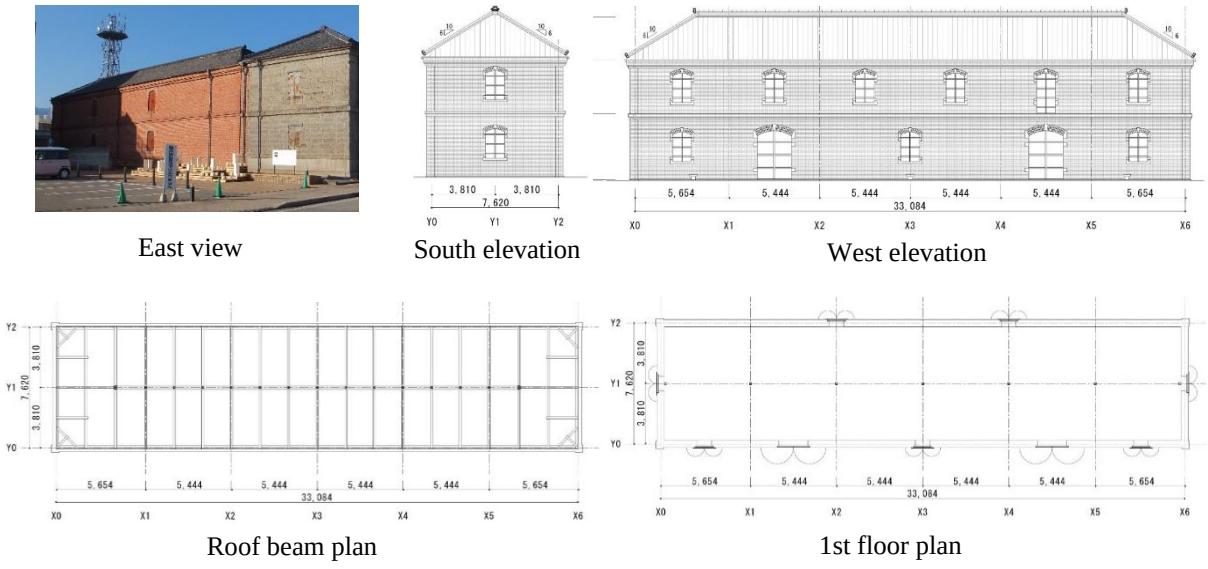

Figure 1: Exterior appearance, plan, section, and elevation of the warehouse

2 MEASUREMENTS AND VIBRATION CHARACTERISTICS

2.1 Measurements and analyses

Micro-tremor observations and excitation tests were carried out to identify natural frequencies and vibration modes of the structure. Servo-type accelerometers of sensitivity 0.3V/(m/s^2) were used with 16-bit data recorder at 1/256 sec sampling and 0.01 V range. The exciter was a linear motor type with a moving mass of 50 kg. The representative locations of accelerometers and the exciter are depicted in Figure 2.

Micro-tremor was measured for 20 minutes and divided into twenty samples of 1 minute, then calculated spectra were ensemble averaged to deduce the transfer functions via FFT. The exciter was operated by two rounds of ascending and descending logarithmic sweep signals from 1 Hz to 30 Hz for two minutes in total. Four of 30 seconds of one-way log-sweep samples were used for the transfer function similar to micro-tremor data. The transfer functions are calculated by H_1 definition, i.e. square norm of cross spectrum divided by products of square roots of auto spectra.

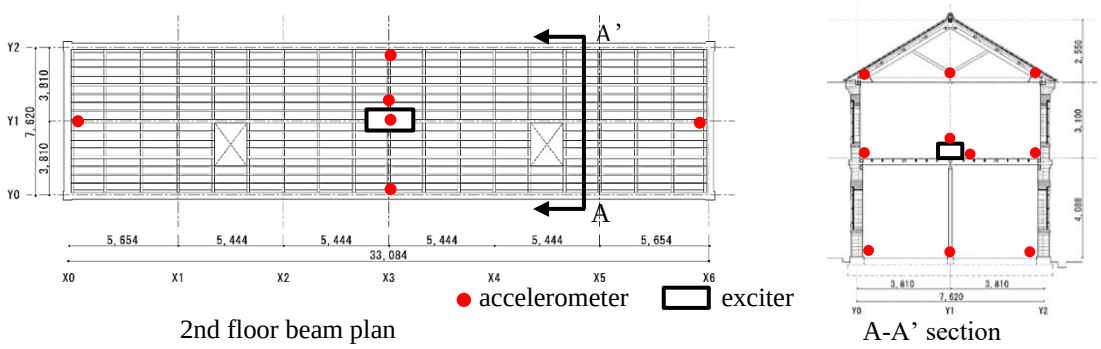

Figure 2: Location of accelerometers and an exciter

2.2 Micro-tremor measurements

Acceleration wave forms and Fourier amplitudes at the center of the 1st floor are shown in Figure 3 for longitudinal and transverse directions. The predominant frequency of 10 Hz is attributable to the reverberation of the subsurface ground.

In Figure 4, transfer functions at the roof level and the 2nd floor level are shown in both directions referring to the 1st floor level. For the transverse direction, the 1st peak at the fundamental frequency 1.95 Hz is followed by several peaks at 4.43, 5.53, 6.87, and 8.37 Hz. Around 5.53Hz and 8.37 Hz, phase relations imply that the corresponding peaks are non-local shear vibration modes. For the longitudinal direction, limited number of peaks are observed. The fundamental frequency is deduced as 7.47 Hz.

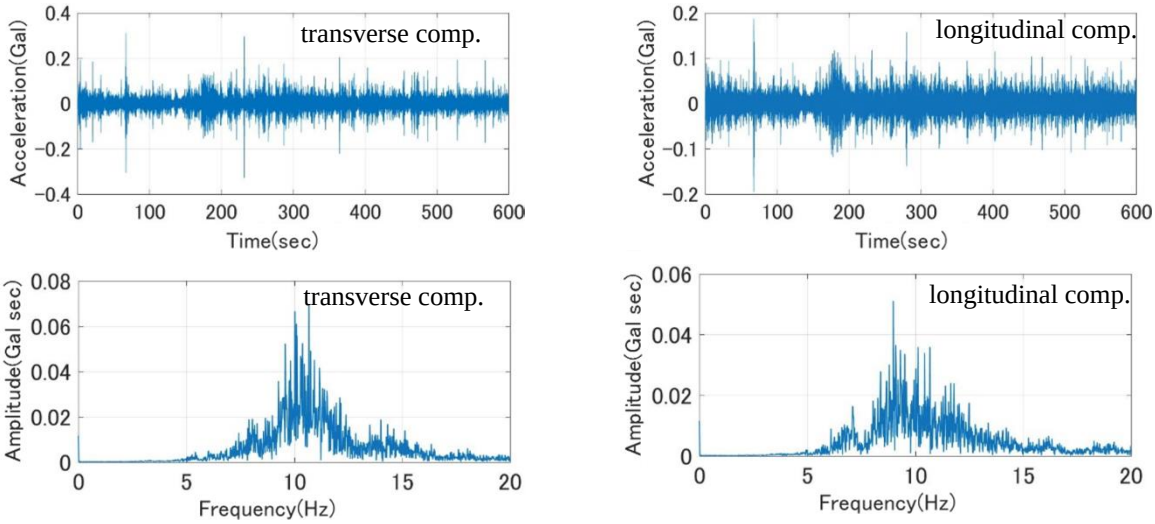

Figure 3: Micro-tremor at the center of the 1st floor

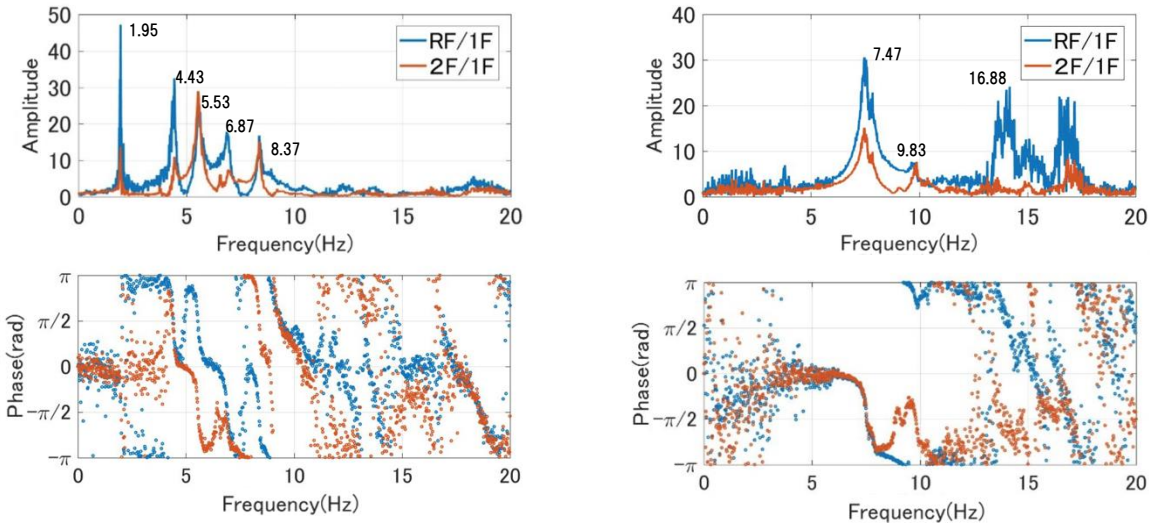

transverse comp. longitudinal comp.

Figure 4: Transfer functions by micro-tremor at the center of the floors

2.3 Excitation by an exciter

The waveform and Fourier amplitude of the log-sweep force are shown in Figure 5. In Figure 6, resonant curves are compared at the roof and the 2nd floor levels. For the transverse direction, the fundamental frequency is 2.03 Hz and the major peaks with resonated phase are seen at 6.00 Hz and 8.63 Hz. In the longitudinal direction, the 1st peak at 7.43 Hz is not dominated and followed by peaks at 10.57Hz and 16.50 Hz.

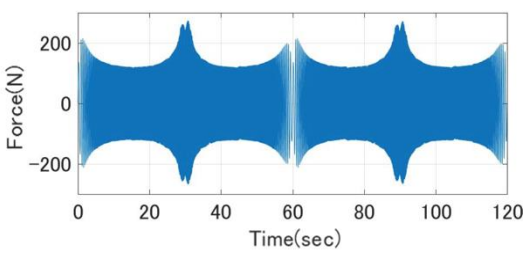

Waveform of log-sweep force

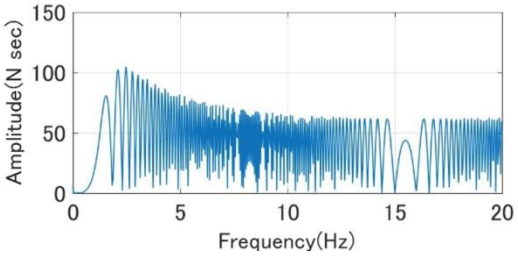

Fourier amp. of log-sweep force

Figure 5: Excitation force at the center of the 2nd floor

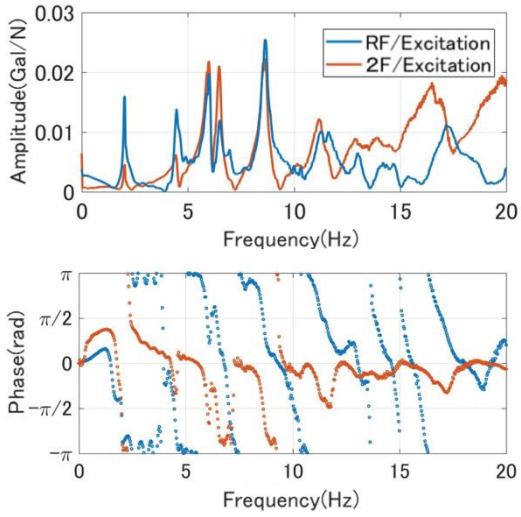

transverse comp.

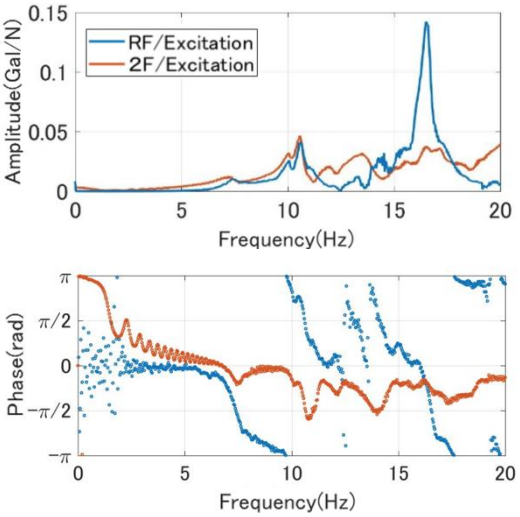

longitudinal comp.

Figure 6: Resonant curves for excitation at the center of the 2nd floor

2.4 Comparison of peak frequencies

Peak frequencies obtained by micro-tremor observation and excitation tests are compared in Figure 7. They are mostly corresponding with each other, which implies that this small size exciter is effective in obtaining resonant curves of this stiff and heavy masonry structure.

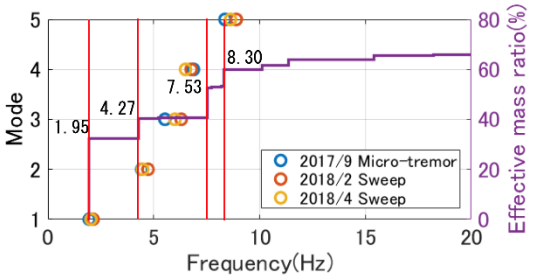

transverse comp.

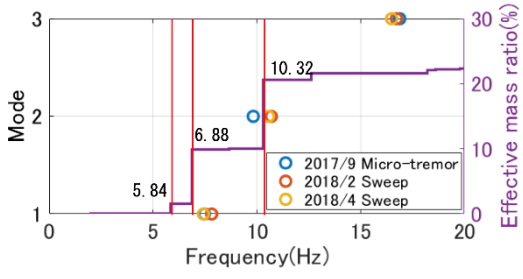

longitudinal comp.

Figure 7: Summary of peak frequencies by measurements and accumulated effective mass ratio by FEM

3 OVERALL FEM MODEL

3.1 Finite element modeling and validation

The finite element model for the masonry warehouse was constructed by combination of isotropic solid elements and beam elements; the former for brick walls and the latter for wooden beams, columns and roof construction. Material constants for beam elements are referred to that of red pine wood obtained by the material test for this project. Poisson's ratio and density for solid elements are typical value for bricks, and Young's modulus for solid elements are set to fit the fundamental frequency of 1.95 Hz in the transverse direction. Damping ratio is 2 %. These material constants are summarized in Table 1. The finite element model is shown in Figure 8. Variation of wall thickness is modelled according to the actual wall configuration as shown in the figure.

Effective mass ratios for natural modes are plotted for natural frequencies and compared with the peak frequencies obtained by micro-tremor observation and excitation tests in Figure7. Peak frequencies are mostly corresponding to the large effective mass ratio.

Table 1: Material constants for brick solid element and wood beam element

	Young's modulus [N/mm^2]	Poisson's ratio	Mass density [g/cm^3]
Brick	2,310	0.2	1.67
Wood	11,830	0.4	0.57

3.2 Simulation analysis (phase in excitation test)

Transfer functions referred to the 1st floor are calculated by time domain FEM linear analysis in each direction as shown in Figure 9. Input acceleration is a 128 sec. portion of measured micro-tremor data on the 1st floor as shown in Figure 3. Similar results for the excitation test are shown in Figure10 where the measured excitation force is used as an input. Comparing these transfer functions with the corresponding experimental ones in Figure 4 and Figure 6, the FEM simulation in the transverse direction is effective up to 5 Hz covering the 1st and 2nd peaks, and in the longitudinal direction up to 10 Hz including the 1st peak.

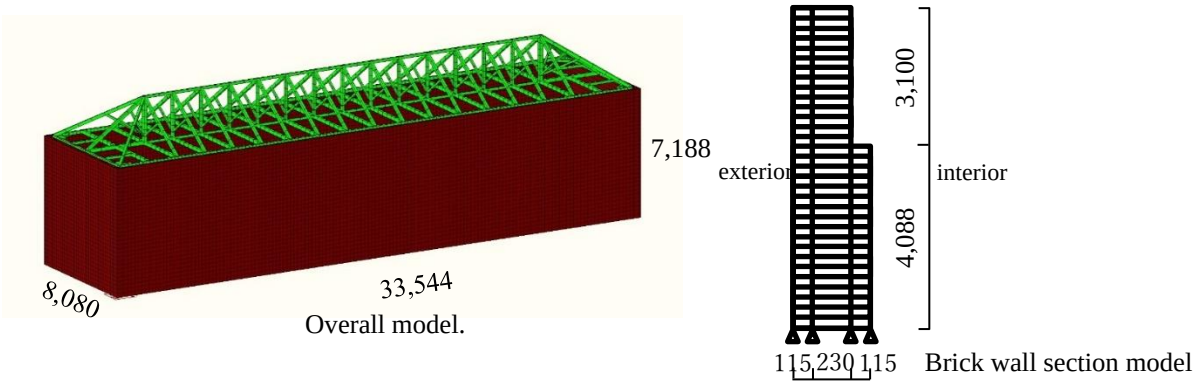

Figure 8: Overall FEM model

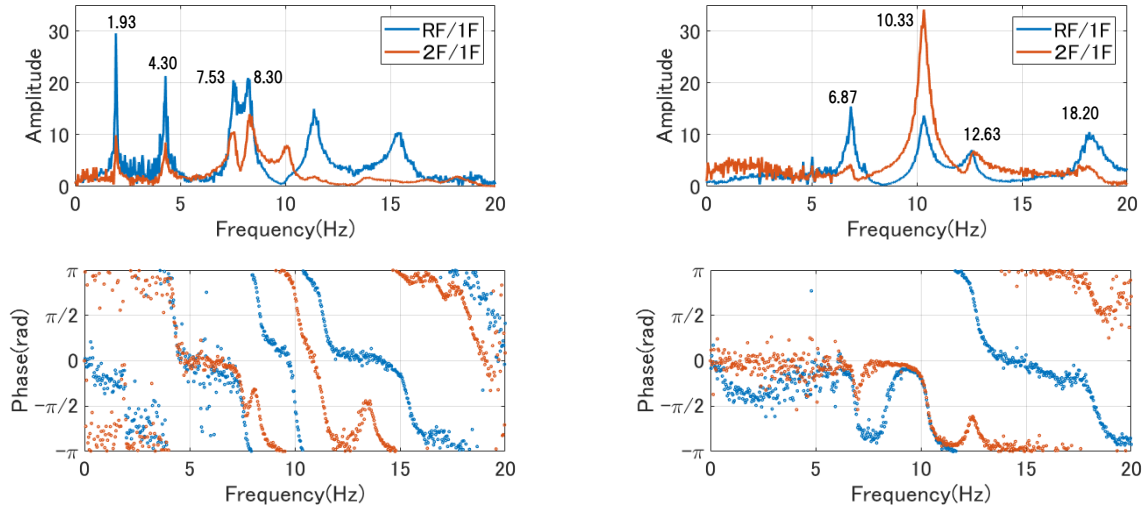

transverse comp. longitudinal comp.

Figure 9: Transfer functions for micro-tremor by FEM

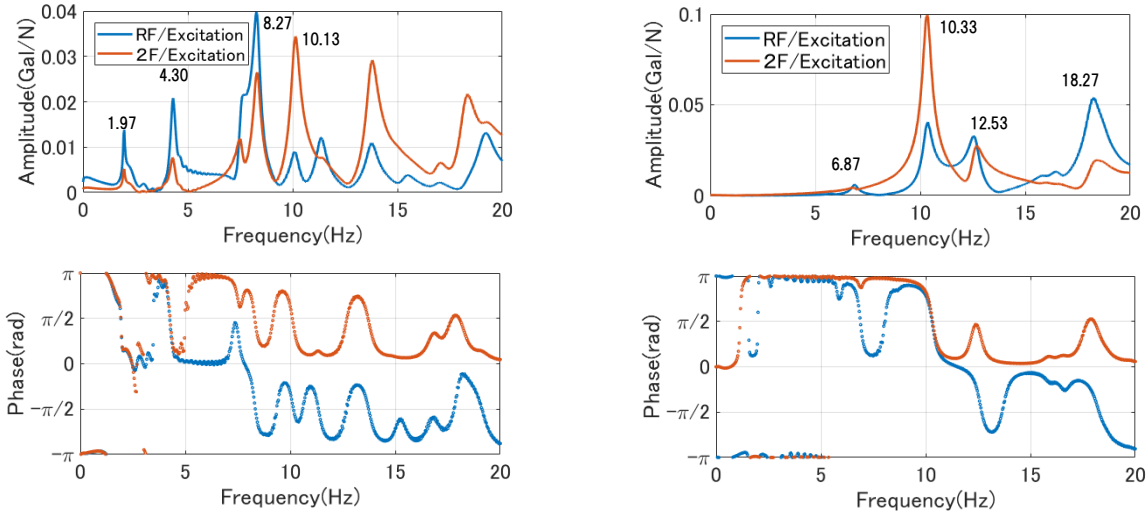

transverse comp. longitudinal comp.

Figure 10: Resonant curves for exciter on the 2nd floor by FEM

3.3 Linear static and dynamic stress analyses

Following the shear coefficient design procedure in Japan, static earthquake load corresponding to the base shear coefficient of 0.2 is applied to the finite element model in each direction. In Figure 11, the distributions of deformation, von Mises stress, and relevant stress components are depicted in transverse direction. Deformation is large in the middle of the roof construction and edges of walls nearby. Normal stress σ_{zz} is dominant at the bottom of the longer brick wall due to the out-of-plane bending at the foot of the wall. Membrane shear stress σ_{xz} near the upper corners of the longer brick wall is remarkable.

In Figure 12, these distributions are shown for longitudinal direction. Similar trends are seen in σ_{zz} and σ_{yz}, but not that remarkable. Then, we will focus on behavior in transverse direction hereafter. Stress distribution in the longer wall is similar to that of a gravity-loaded plate with three edges fixed; since base and perpendicular shorter walls play roles of constraints along the three edges of the longer wall. With the same finite element model, a dynamic analysis was carried out with Kobe NS component ground motion in 1995 as shown in Figure 13. The distributions of maximum absolute stress shown in Figure 14 are similar to that of the static loading.

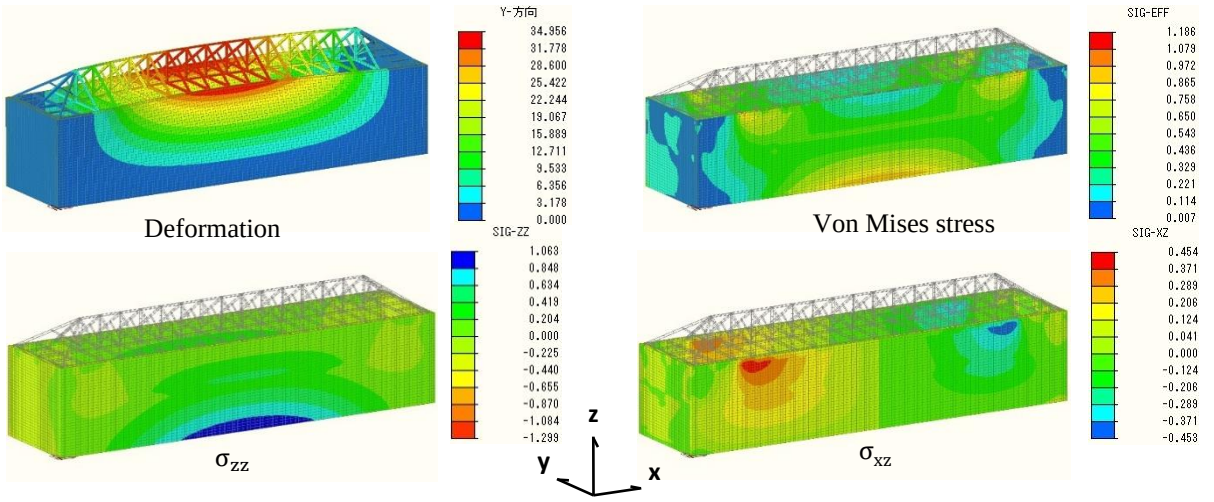

Figure 11: Distribution of deformation and stress components for static load in transverse direction

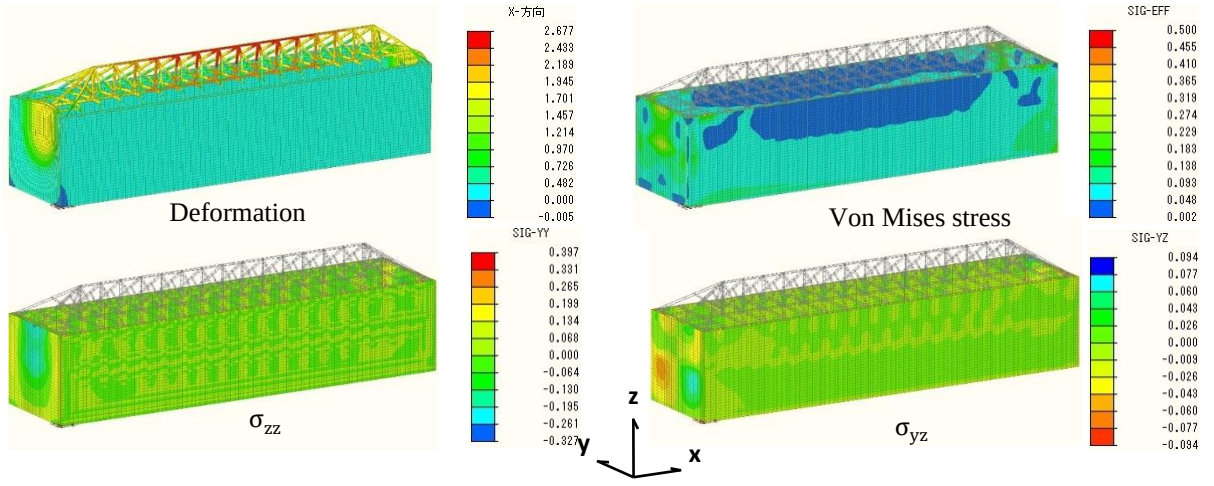

Figure 12: Distribution of deformation and stress components for static load in longitudinal direction

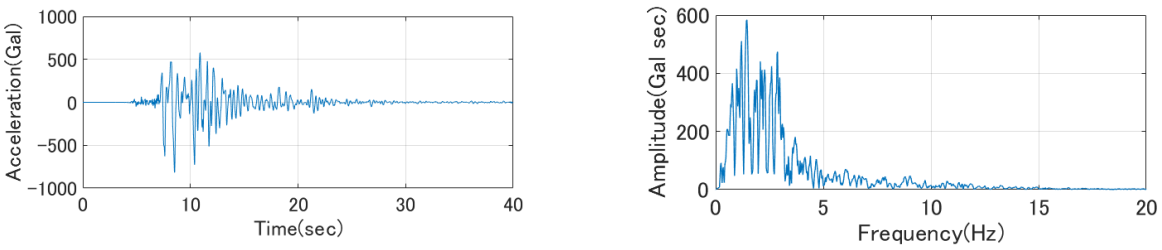

Figure 13: Waveform and Fourier spectrum of input wave, Kobe 1995

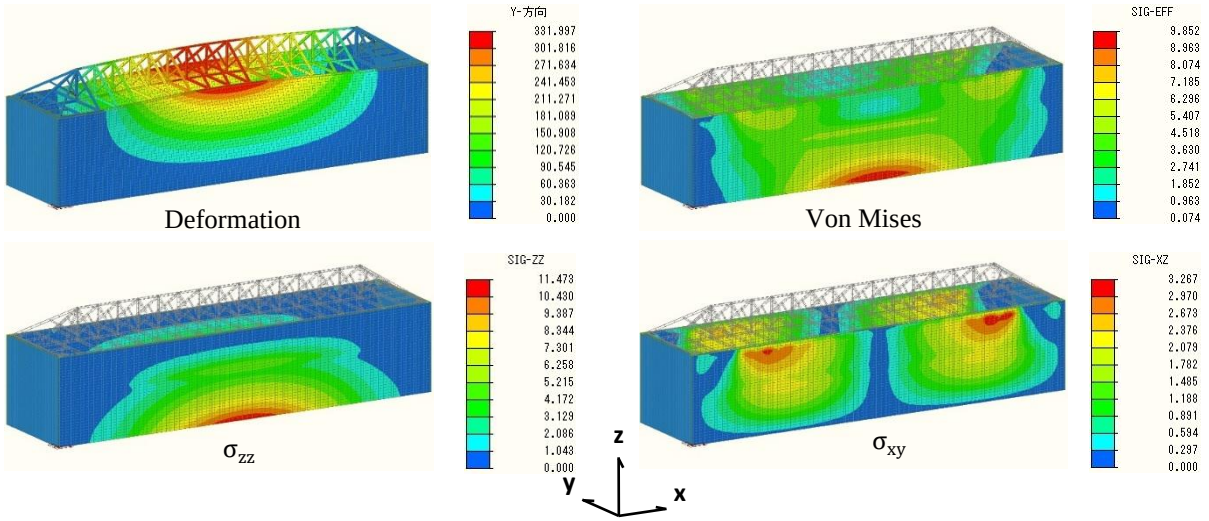

Figure 14: Maximum deformation and stress for Kobe ground motion in transverse direction

4 LOCAL DEM MODELS

4.1 Finite element model and the local discrete element models

Strength of brick wall is governed by the shear strength of its joint. Shear strength and tensile strength of brick joint is much weaker than compressional strength, usually assumed as 1/10 of compressional strength. For the loading in transverse direction, tensile stress at the center bottom and shear stress around upper corners of the longer wall are most significant.

After local crack develops along the joints, brick walls are regarded as discontinuous structure. DEM is a powerful tool to analyze discontinuous structure; the structure is modeled by a set of rigid blocks or deformable blocks moving with each other under external forces and contact conditions. However, it requires long time of computation with large amount of memory to evaluate contact between tremendous number of DOF's of blocks in a three-dimensional discontinuous model. It may be advantageous to incorporate three-dimensional FEM and two-dimensional DEM to predict crack expansion in certain parts of the structure during earthquake ground motion.

We set two DEM local models; one for at the center bottom of the longer wall and the other at the upper edge near the corner of the longer wall as shown in Figure 15. The former model is a part of the wall section modeled by plane strain and designated as bending model. The latter

model is a part of the wall modeled by plane stress and designated as shear model. Both local models are modeled by a set of rigid blocks with normal and shear contact springs along their edges. The normal spring is used to prevent penetration and the shear spring to evaluate shear stress to be used for slip criteria. Contact strengths at interfaces are defined by tensile strength and slip criteria expressed by cohesion and friction angle shown in Table 2. Mass density of blocks is 1.66g/cm^3.

The input motion for the DEM models are the displacements calculated by FEM dynamic analysis. The motion is specified at the peripheries of the DEM models, where special blocks called by the periphery blocks are equipped. The periphery blocks are expressed by double lines along the edges in Figure 16 and Figure 17. Normal contact spring coefficients are assumed by Young's modulus of the brick divided by distance between adjacent block centers as shown in Table 3. Shear contact spring coefficient is specified as 0.0353 N/mm^3, according to the Young's modulus of joint material. Shear and normal contact springs for the periphery blocks are parametrically assumed as 10N/mm^3, 1N/mm^3, and 0.1N/mm^3. In this paper, the result for 10N/mm^3 are shown for space limitation.

Table 2: Strength for brick solid elements

	Tensile strength [N/mm^2]	Cohesion [N/mm^2]	Friction angle [degree]
Interior interface	0.45	0.52	33
Periphery interface	10,000	10,000	89

Table 3: Normal contact spring coefficients for horizontal and vertical joints [N/mm^3]

	Horizontal joint	Vertical center joint	Vertical off-center joint
Bending model	34.48	10.04	13.39
	Horizontal joint	Vertical for long face	Vertical for short face
Shear model	34.48	20.09	10.04

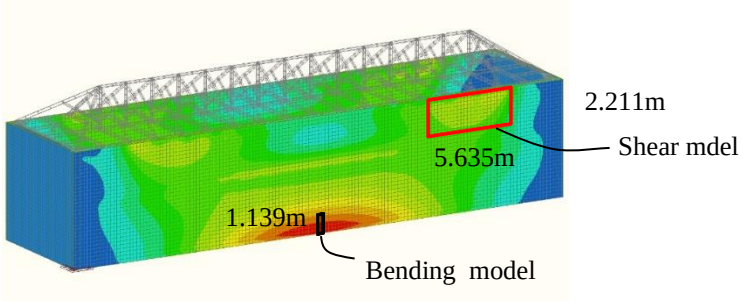

Figure 15: Locations of local DEM models

4.2 Plane strain analysis for bending model

In Figure16, development of cracks at joints in the wall section is shown for the case of 10N/mm^3 periphery block contact spring. Firstly, horizontal cracks appear at the outer face then at the inner face; cracks appear alternatively at both faces while proceeding to interior region and finally several joints penetrating whole thickness of the wall. Cracking pattern depends on

the periphery block contact spring; crack concentration at the middle of the wall for 1N/mm^3 and less cracking for 0.1N/mm^3 (not shown here). The cracking pattern for 10N/mm^3 suits to the summary of empirically inferred collapse mechanism for masonry walls [4].

4.3 Plane stress analysis for shear model

In Figure17, development of cracks at joints on the wall is shown for the case of 10N/mm^3 periphery block contact spring. Crack patterns comprises vertical and diagonal cracks; the vertical cracking is proceeding downward from near the corner of the wall, while the diagonal cracking is proceeding from the lower left corner toward the upper right corner. Similar to the bending model, cracking is less observable for the smaller periphery block contact spring (not shown here).

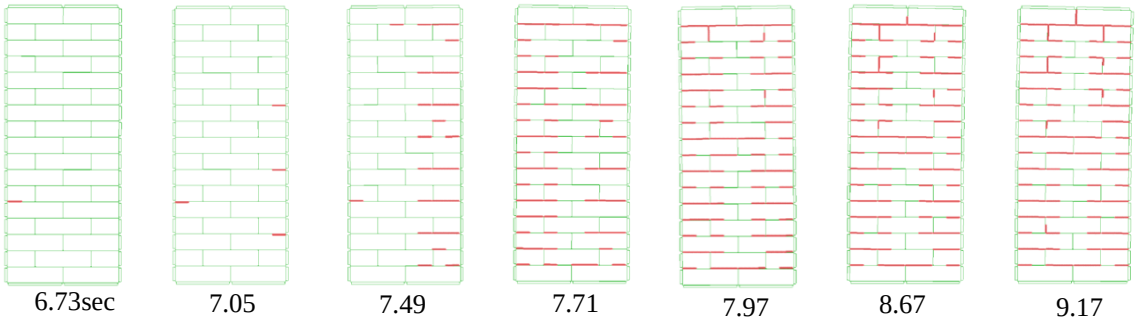

Figure 16: Development of cracks in local bending model for specified motion computed by FEM

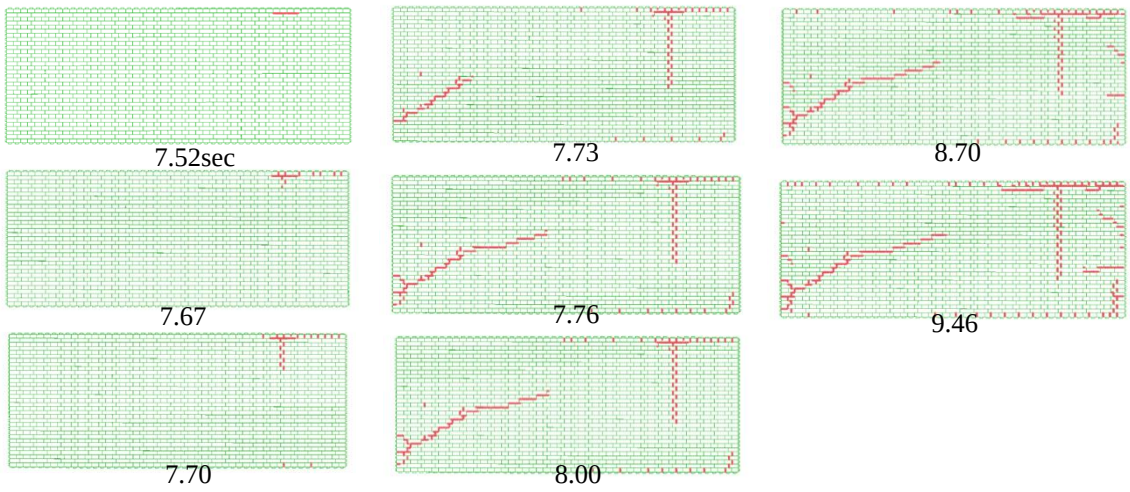

Figure 17: Development of cracks in local shear model for specified motion computed by FEM

5 CONCLUSIONS

Collapse mechanisms of a two-story brick masonry warehouse with wooden frame reinforcements, which is a typical heritage structure in the opening era of the modern Japan, was studied for strong earthquake ground motion by coupling three-dimensional finite element

analysis and two-dimensional discrete element analysis. Three-dimensional vibration characteristics revealed by micro-tremor observation and an exciter test were simulated by a three-dimensional overall FE model; where stiffness of wooden roof and wooden 2nd floor structures were examined for higher vibration modes. The FE analyses for static horizontal load and dynamic ground motion exhibited dominating bending stress at the centre bottom and dominating membrane stress at the upper corners of the longer wall for the transverse excitation. The latter stress distribution is similar to that of a gravity loaded plate with three-edge constraints, since the perpendicular shorter walls function as constraints for the longer walls.

By two-dimensional DEM local models, the dominating bending stress was analysed by plane strain and the dominating membrane stress by plane stress. For both models, time-varying dynamic displacement response obtained by the three-dimensional FE model were specified at their peripheries with periphery contact springs to control the boundary stiffness. At the centre bottom of the wall, DEM revealed that the joint splitting was developing horizontally in the section. At the upper corners, joint splitting was proceeding obliquely on the wall. These collapse mechanisms are in accordance with the summary of empirically inferred collapse mechanism for masonry walls.

Acknowledgements. This paper is based on the 2nd author's Master's Thesis of Waseda University in 2018. This paper is a part of the outcome of research performed under a Waseda University Grant for Special Research Projects (Project number: 2018B-127).

REFERENCES

[1] Hironaka, T., Maeda, T. Araya, M. and Ejiri, N. Safety Evaluation of Inner Gallery in Bayon Temple by DEM with Preliminary Experiments, *10th SAHC* (2016).
[2] Yamashita, Y. and Maeda, T. Simulation of Distinct Element Joint Stiffness of the Historical Masonry Structure Model by Micro-tremor Measurement, *11th SAHC* (2018).
[3] Yamamoto, T. and Maeda, T. Earthquake Safety Assessment of a Tall Brick Chimney in Tokoname Based on the Micro-Tremor Measurement, *14WCEE* (2008), 05-04, 0073.
[4] Minamide ,K. et al. Basic investigation of seismic diagnosis method on historical masonry, Historical masonry prevention committee's report, *Proceedings of Annual meeting for Hokkaido Branch of Architectural Institute of Japan*, (1997), pp.253-256 *in Japanese*.